On the possibility of time-lapse ultrahigh-resolution optical coherence tomography for bladder cancer grading

Zhijia Yuan, Bai Chen, Hugang Ren, and Yingtian Pan*
State University of New York at Stony Brook, Department of Biomedical Engineering, Stony Brook, New York 11794

Abstract. It has been recently demonstrated that the cellular details of bladder epithelium embedded in speckle noise can be uncovered with time-lapse ultrahigh-resolution optical coherence tomography (TL-uOCT) by proper time-lapse frame averaging that takes advantage of cellular micromotion in fresh biological tissue *ex vivo*. Here, spectral-domain 3-D TL-uOCT is reported to further improve the image fidelity, and new experimental evidence is presented to differentiate normal and cancerous nuclei of rodent bladder epithelia. Results of animal cancer study reveal that despite a slight overestimation (e.g., $<$10%) of nuclear size (D_N) to histological evaluation, TL-uOCT is capable of distinguishing normal ($D_N \approx 7\ \mu$m) and cancerous (e.g., high-grade $D_N \approx 13\ \mu$m) urothelia, which may potentially be very useful for enhancing the diagnosis of nonpapillary bladder cancer. More animal study is being conducted to examine the utility to differentiate hyperplasia, dysplasia, and carcinoma *in situ*.
[DOI: 10.1117/1.3223246]

Keywords: Coherent optics; imaging systems; biomedical optics.

Paper 09111LRR received Mar. 26, 2009; revised manuscript received Jul. 9, 2009; accepted for publication Jul. 14, 2009; published online Sep. 16, 2009.

Confocal microscopy (including optical coherence microscopy, or OCM[1,2]) and multiphoton microscopy permit subcellular imaging of superficial biological tissue such as skin, oral, and cervical epithelia; however, these techniques require high NA objective and focal tracking to provide subcelullar images at different depths, which may pose a technical challenge for endoscopic *in vivo* diagnosis. On the other hand, optical coherence tomography (OCT) is a coherence-gated technique that enables sub-10-μm cross-sectional imaging of biological tissue.[3] As the axial resolution is defined by the source coherence length $L_c \approx 0.44\lambda^2/\Delta\lambda$ (assuming a Gaussian line shape; λ, $\Delta\lambda$: central wavelength, spectral bandwidth), ultrahigh-resolution OCT (uOCT) with $L_c < 1$ to 2 μm is possible by employing a broadband source and subcellular imaging of translucent tissue—e.g., *xenopus laevis*—has been reported,[4,5] However, subcellular uOCT (not OCM) of scattering mammalian tissue (e.g., epithelium) remained unsolved, preventing the use of this promising technique to render optical biopsy for clinical diagnosis. Interestingly, time-domain (TD) time-lapse uOCT (TL-uOCT), taking advantage of cellular micromotion in fresh *ex vivo* tissue for effective speckle noise reduction, was recently demonstrated to uncover the subcellular details (i.e., nuclei) in bladder epithelium using a low-NA commercial achromatic lens (f 10 mm/NA 0.25).[6] In this letter, we present spectral-domain (SD) TL-uOCT to further enhance image contrast and resolution and enable 3-D subcellular imaging and provide new experimental data to evidence the possibility for epithelial cancer grading.

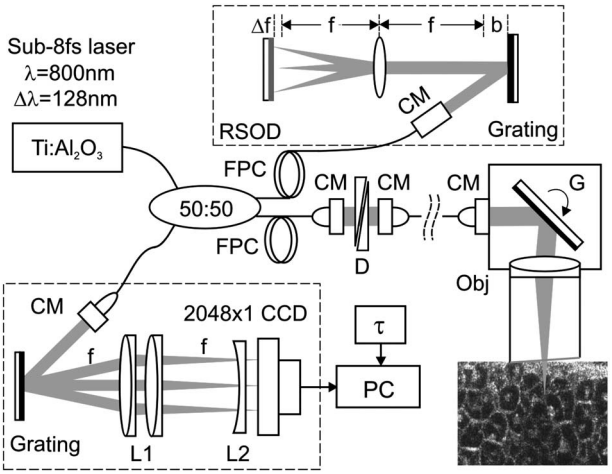

Fig. 1 Schematic of SD TL-uOCT. CM: fiber-optic collimator; FPC: fiber polarization controller; D: BK7 wedge prism pair; RSOD: grating-lens-based rapid optical delay for dispersion compensation; G: servo mirror; Obj: achromatic lens (f 10mm/NA 0.25); τ: delay trigger for TL-uOCT; L1, L2: achromatic lens group for field correction.

Figure 1 illustrates an SD TL-uOCT setup for subcellular bladder imaging, in which an ultrafast $Ti:Al_2O_3$ laser (λ = 800 nm, $\Delta\lambda_{FWHM}$ = 128 nm) was employed to illuminate a wavelength-flattened fiber-optic Michelson interferometer. In the reference arm, light exiting the fiber was collimated to ϕ2 mm and connected to a grating lens rapid scanning optical delay (RSOD, d^{-1} = 1200/mm, f = 80 mm) for matching the path length and dispersion between the two arms of the interferometer. Light in the sample arm was collimated by a fiber-optic achromate to ϕ5 mm, scanned laterally by two-axis servo mirrors, and focused by a commercial-grade achromatic lens (f 10 mm/NA 0.25) onto the bladder epithelium under examination, yielding a measured focal spot (lateral resolution) of $\sim\phi 3\ \mu$m. The backscattering from within the bladder wall was recombined with the reference light in the detection fiber and connected to a spectral imager in which the light was collimated by a fiber-optic achromate (f = 55 mm), diffracted by a holographic grating (d^{-1} = 1200/mm), and focused by a lens system (f = 85 mm) onto a line CCD camera ($10 \times 10\ \mu m^2$/pixel). Each captured interferometric spectrograph was transferred to a PC via a Camera Link interface at 100 MB/s and processed to reconstruct the corresponding

*Tel: 631-444-1451; E-mail: yingtian.pan@sunysb.edu

1083-3668/2009/14(5)/050502/3/$25.00 © 2009 SPIE

depth profile (i.e., A-scan), permitting 2-D uOCT at up to 50 fps. Optimizing the L_c of uOCT was achieved by spectral reshaping using RSOD in the reference arm and fiberoptic polarization controllers (FPC) to maximize the bandwidth of the modulation cross-spectrum (e.g., $\Delta\lambda \geqslant 155$ nm); this procedure was found much easier to implement than in previously reported TD uOCT.[6] Mismatch of dispersion between the two arms was coarsely adjusted by RSOD, wedge prisms, and FPC (for polarization-mode dispersion) and then fully compensated numerically,[7] which ensured an axial resolution approaching the transform limit, i.e., $L_c = 2.3$ μm or 1.7 μm in bladder tissue (refractive index $n \approx 1.37$ is assumed).

TL-uOCT, based on time-lapse frame averaging of dynamic cellular backscattering, has been shown to effectively reduce speckle noise and uncover subcellular details in fresh urothelium *ex vivo*.[6] SD uOCT, owing to its improved image sensitivity and frame rate, can further enhance time-lapse phase scrambling (speckle removal) for subcellular delineation and thus potentially enable 3-D TL-uOCT. The detected TL-uOCT signal can be simplified by ensemble averaging of snapshots of uOCT signal $I_{uOCT}(L_r)$:

$$I_{TL\text{-}uOCT}(L_r) = \sum_{\tau} I_{uOCT}(L_r)/N_\tau = (1/N_\tau)\sum_{\tau} 2I_r^{1/2}\sum_{i} E^b(L_{s,i})\exp[-4(L_{s,i} - L_r)^2/L_c^2]\cos[k(L_{s,i} - L_r)], \quad (1)$$

where N_τ is the total times of τ-delayed frame averaging. $E^b(L_{s,i})$ is the backscattering from an intracellular organelle at a path length expressed as $L_{s,i} = L_{s0} + \Delta L_{s,i}$ to analyze the effects of two types of motion on speckle dynamics. The motion of L_{s0} (origin, e.g., center of a nucleus) pertains to translation of cell matrix (tissue), which can be compensated by image registration and might otherwise blur the τ-lapse averaged image. $\Delta L_{s,i}(t)$ is attributed to intracellular relative motion of living cells essential to TL-uOCT. For a snapshot, $\Delta L_{s,i}$ is stationary, and the summation $(\Sigma_i \cdot \cdot)$ of all backscattering $E^b(L_{s0} + \Delta L_{s,i})$ constitutes a speckle pattern $I_{uOCT}(L_r)$. However, intracellular motion over time τ scrambles the phase $k\Delta L_{s,I}(\tau)$; thus, time-lapse averaging $\Sigma_\tau I_{uOCT}(L_r)$ can reduce the speckle noise and uncover the embedded subcellular details (e.g., nucleus). Noteworthily, L_{s0} may not be completely compensated by image registration (e.g., moving out of focus or image plane); thus, a proper time-lapse τ (e.g., $\tau \approx 0.1$ to 0.7 s) is a compromise between image blurring and sufficient phase scrambling for speckle noise reduction.

Figure 2 compares a snapshot of a uOCT image (a) of a fresh rat bladder *ex vivo* acquired at 50 fps showing no resolvable cellular morphology due to speckle noise and a TL-uOCT image (b) that uncovers subcellular details, e.g., the nuclei N ($D_N = 6.9 \pm 0.5$ μm) of rat urothelium ($\tau \approx 0.15$ s). Compared with TD TL-uOCT, the image fidelity for nuclear delineation is markedly enhanced and the effective imaging depth is increased (e.g., >500 μm) to the upper *muscularis* of the bladder wall without focal tracking. Figure 3 further demonstrates the 3-D subcellular imaging capability of TL-uOCT owing to the enhanced temporal resolution of SD uOCT. Ten slices of 2-D SD uOCT were acquired each time and were repeated 10 times for time-lapse frame averaging

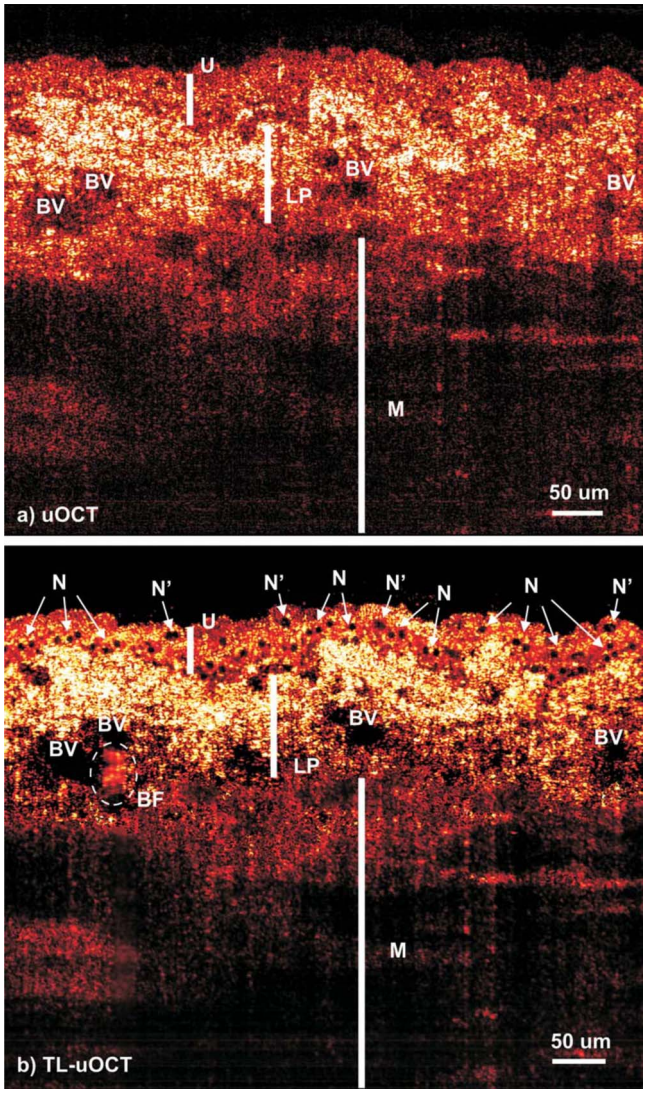

Fig. 2 Fresh Sprague-Dawley rat bladder *ex vivo*. (a) Snapshot; (b) TL-uOCT image ($N_\tau = 10$, $\tau \approx 0.15$ s). U: urothelium; LP: *laminar propria*; M: *muscularis*;. N: nuclei ($D_N \approx 6.9$ μm); N′: umbrella-cell nuclei ($D_N \approx 13$ μm).

($N_\tau \approx 10$, $\tau \approx 0.2$ s). To further examine the utility of this technique in the diagnosis and grading of epithelial cancers, a transgenic mouse model was used to provide orthotropic bladder cancers. Figure 4 compares the results of TL-uOCT and the corresponding histology. For normal mouse bladder (a), TL-uOCT was able to resolve the nuclei of the urothelium and delineate the underlying bladder morphology (e.g., *lamina propria*, *muscularis*) without focal tracking. The nuclear size measured by TL-uOCT ($D_N = 6.7 \pm 1.1$ μm) well matched that of histology ($D_N = 6.0 \pm 0.8$ μm). In contrast, the structural heterogeneity in the cancerous lesion (b) was markedly increased, resulting in reduced OCT imaging depth, consistent with our clinical observations using endoscopic OCT. More importantly, TL-uOCT was able to track the increase of the nuclear size to $D_{N''} = (12.9 \pm 1.3)$ μm in the bladder tumor; this measurement based on the 10 sampled nuclei ($N''_1 - N''_{10}$) closely matched the histological counterpart of $D_{N''} = (11.7 \pm 0.9)$ μm. This lesion was later confirmed histologi-

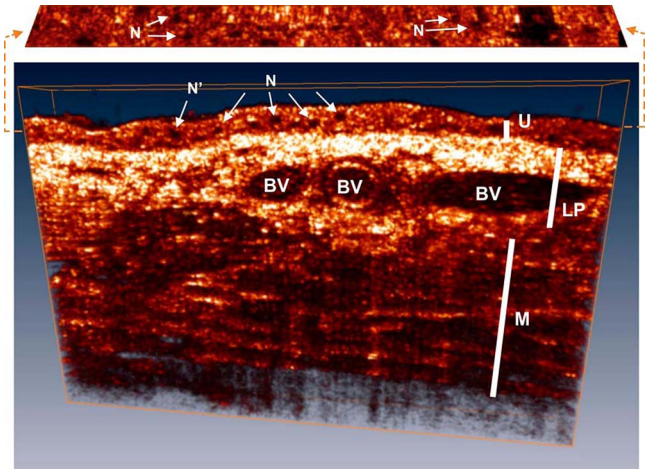

Fig. 3 Three-dimensional TL-uOCT of a fresh rat bladder *ex vivo* (N_τ=8, $\tau\approx$0.2 s). 3-D image size: 500×265×40 μm^3 (10 slices). The upper panel is the *en face* image within the urothelium as indicated by two dashed lines. N: nuclei (D_N=7.4±0.8 μm); N′: umbrella-cell nuclei ($D_{N'}\approx$11 μm).

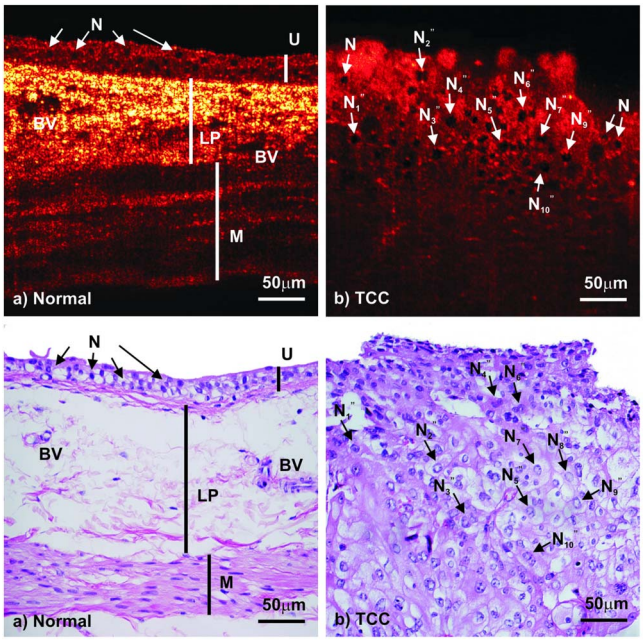

Fig. 4 Subcellular TL-uOCT of fresh mouse bladders *ex vivo* compared with the corresponding histology. (a) Normal bladder (N_τ=4, $\tau\approx$0.32 s); (b) transitional cell carcinoma or TCC (N_τ=4, $\tau\approx$0.4 s). Nuclear sizes measured by TL-uOCT/histology were (a) D_N =(6.7±1.1) μm/(6.0±0.8) μm for normal urothelium (b) and D_N =(12.9±1.3) μm/(11.7±0.9) μm for high-grade (G3) TCC.

cally as a high-grade (G3) urothelial cancer or transitional cell carcinoma.

In summary, we present an SD TL-uOCT technique to further enhance subcellular imaging of epithelial tissue. The key is to enhance local cellular-motion-induced phase scrambling while minimizing global motion (translation or shift), e.g., by image registration. Apparently, the higher detection SNR and imaging rate (temporal resolution) of the spectral-domain approach enables more effective speckle reduction for subcellular delineation and 3-D subcellular imaging. Results of the animal cancer model study confirmed that TL-uOCT measurements of urothelial nuclei closely matched those of the corresponding histology. More importantly, this technique was able to track the nuclear enlargement in cancerous lesions, thus demonstrating the potential for direct epithelial cancer grading. It is important to note that as TL-uOCT uses a low-NA achromatic lens (f 10mm/NA 0.25), it enables imaging of subcellular details in the epithelium and the underlying morphology of bladder wall over 0.5 mm of depths without focal tracking; thus, it is potentially suitable for endoscopic optical or optically guided biopsy of carcinoma *in situ* where cancer grading is crucial. Noteworthily, motion artifacts induced by more vigorous bladder contraction and handshaking in clinical OCT cystoscopy could be more challenging for TL-uOCT than the *ex vivo* studies presented here, but we have found in our clinical trials that motion artifacts can be dramatically reduced by contacting the OCT scope tip with the bladder wall. Development and test of a microelectrochemical systems (MEMS)–based endoscopic TL-uOCT is being conducted to transform the current handheld device to a rigid endoscopic setting for *in vivo* subcellular imaging of bladder cancer.

Acknowledgments

This work was supported in part by NIH Grant No. R01DK059265 and Fusion Award.

References

1. S. Tang, C. H. Sun, T. B. Krasieva, Z. P. Chen, and B. J. Tromberg, "Imaging subcellular scattering contrast by using combined optical coherence and multiphoton microscopy," *Opt. Lett.* **32**, 503–505 (2007).
2. S. W. Huang, A. D. Aguirre, R. A. Huber, D. C. Adler, and J. G. Fujimoto, "Swept source optical coherence microscopy using a Fourier domain mode-locked laser," *Opt. Express* **15**, 6210–6217 (2007).
3. D. Huang, E. A. Swanson, C. P. Lin, J. S. Schuman, W. G. Stinson, W. Chang, M. R. Hee, T. Flotte, K. Gregory, C. A. Puliafito, and J. G. Fujimoto, "Optical coherence tomography," *Science* **254**, 1178–1181 (1991).
4. W. Drexler, "Ultrahigh-resolution optical coherence tomography," *J. Biomed. Opt.* **9**, 47–74 (2004).
5. S. A. Boppart, B. E. Bouma, C. Pitris, J. F. Southern, M. E. Brezinski, and J. G. Fujimoto, "*In vivo* cellular optical coherence tomography imaging," *Nat. Med.* **4**, 861–865 (1998).
6. Y. T. Pan, Z. L. Wu, Z. J. Yuan, Z. G. Wang, and C. W. Du, "Subcellular imaging of epithelium with time-lapse optical coherence tomography," *J. Biomed. Opt.* **12**, 0505041–3 (2007).
7. S. Makita, T. Fabritius, and Y. Yasuno, "Full-range, high-speed, high-resolution 1-mm spectral-domain optical coherence tomography using BM-scan for volumetric imaging of the human posterior eye," *Opt. Express* **16**, 8406–8420 (2008).